J. Braz. Chem. Soc., Vol. 5, No. 2, 59-65, 1994.
Printed in Brazil.

© 1994 Soc. Bras. Química
0103 – 5053 $5.00 + 0.00

Photoabsorption Cross Sections of Ar, N_2 and $Si(CH_3)_4$ Derived from Electron Energy Loss Spectroscopy

A.C.A. Souza

Instituto de Química, UFRJ, Cidade Universitária, 21949-900 Rio de Janeiro - RJ, Brazil

*S.K. Srivastava**

Jet Propulsion Laboratory, California Institute of Technology, 4800 Oak Grove Drive, Pasadena, CA 91109, USA

Received: December 29, 1992; June 7, 1994

Utilizando a geometria de feixes cruzados foram obtidos espectros de perda de energia de elétrons (EELS) para Ar, N_2 e $Si(CH_3)_4$ (TMS) a 1 keV e ângulos de espalhamento de 2° a 5°. Os espectros observados foram convertidos em espectros de fotoabsorção utilizando o Teorema do Limite de acordo com o qual, à medida em que a transferência do momento aproxima-se de zero, a força do Oscilador Generalizado (FOG) tende à força do Oscilador Ótico (FOO). As seções de choque de fotoabsorção medidas por este método são relativas e foram posteriormente convertidas a valores absolutos pela normalização a um valor previamente medido num certo comprimento de onda.

Foram obtidas seções de choque para Ar, N_2 na região < 10 eV (130 nm) a 50 eV (15 nm) > e comparadas com dados previamente publicados. A concordância no caso do Ar é excelente e no caso do N_2 satisfatória. Os valores destas seções de choque encontram-se dentro dos limites do erro experimental. Os resultados apresentados servem para mostrar que a técnica de EELS é apropriada para obtenção de seções de choque de fotoabsorção. Para TMS medidas prévias não são prontamente disponíveis. Portanto a normalização foi feita utilizando-se resultados de uma teoria. Os valores normalizados da seção de choque de fotoabsorção entre 4 eV (300 nm) e 100 eV (12,5 nm) são apresentados numa forma tabular.

Utilizing a crossed electron beam-molecular beam collision geometry we have generated electron energy loss spectra (EELS) for Ar, N_2 and $Si(CH_3)_4$ (TMS) at 1 keV electron impact energy and at scattering angles varying from 2° to 5°. These spectra are then converted to photoabsorption spectra by employing the limit theorem, according to which, as the momentum transfer approaches zero the generalized oscillator strength approaches the optical oscillator strength. The photoabsorption cross sections measured by the present method are relative in nature, and are converted to absolute values by normalization to some previously measured value at one wavelength. Cross section values have been obtained for Ar and N_2 in the wavelength region between < 10 eV (130 nm) and 50 eV (15 nm) >, and are compared with previously published data. The agreement in the case of Ar is excellent and for N_2 it is satisfactory. The cross section values are within the error limits of individual experiments. Present results show that the technique of EELS is capable of yielding accurate values of photoabsorption cross sections. Recently published results for TMS in the wavelength range of 55 nm to 95 nm have been used to generate photoabsorption cross sections for the wavelength region from about 12 nm to 206 nm.

Keywords: *photoabsorption, argon, nitrogen, tetramethylsilane*

Introduction

Recently there has been a great interest in the collision and photoabsorption properties of molecules employed in the deposition and etching of semiconducting materials. $Si(CH_3)_4$ (TMS) is one of the candidate molecules for this purpose. This motivated us to measure its photoabsorption properties by utilizing the well known technique of energy loss spectroscopy based on zero momentum transfer pioneered by Lassettre[1] and his co-workers. In order to check

the reliability of results obtained by using our apparatus we first measured photoabsorption cross sections of Ar and N_2 and compared them with previously published accurate values. We then used the same apparatus under identical conditions to obtain values of photoabsorption cross sections of TMS for the first time.

In section II the experimental apparatus and method of data reduction are described, and the results are presented in section III.

Experimental Details

Apparatus

The experimental apparatus has been described in our previous publications by de Souza & Souza[2] and Souza *et al.*[3]. Here we will give a brief description. A schematic diagram of the experimental arrangement is shown in Fig. 1. The present instrument employs crossed electron beam-target beam collision geometry in which a monoenergetic beam of electrons crosses a jet of target species at right angles. The sample is introduced into the vacuum chamber as a molecular beam formed by the expansion of the gas through a hypodermic needle. The electron gun is a commercial model which has been modified to allow for the easy replacement of its hairpin tungsten filament. This is necessary to facilitate work with corrosive gases. The electron beam can be continuously tuned from 500 to 1000 eV. The electron current is typically 50 μA with full width at half maximum (FWHM) of about 0.5 eV. The electron gun can be rotated from - 60 to + 60 degrees in steps of 1'. The zero degree angle is determined experimentally by recording spectra on both positive and negative sides. After collision, the scattered electrons are energy selected by the use of a Möllenstedt[4] velocity analyzer or a Wien Filter[5]. For the data presented here only the Möllenstedt analyzer was used.

At the entrance of the analyzer a system of apertures, typically 50 and 200 μm in diameter, is used in order to reduce the background due to backscattered electrons, as well as to avoid any contribution to this background from the primary beam. With this experimental arrangement, the viewing angle of the Möllenstedt analyzer is 0.57 degrees.

Figure 2 shows details on the solid angle subtended by the analyzer[6]. As is clear from the figure the solid angle $\Delta\Omega$ is given by $\pi(\sin\theta)^2$. For $\theta = 0.57°$ subtended by the analyzer at the scattering center, $\Delta\Omega = 3.11 \times 10^{-4}$ sr.

After scattering, the energy selected electrons are detected by a spiraltron which gives rise to an electrical pulse for each detected electron. These pulses are then counted by conventional pulse counting electronics consisting of a pre-amplifier and an amplifier-discriminator. The final pulses are subsequently stored in a multichannel analyzer.

The local magnetic field in the collision region is reduced from 250 mG to 5 mG by the use of three pairs of Helmholtz coils. The electron gun, the gas nozzle and the detector are housed inside a vacuum chamber. The base pressure of the system is on the order of 10^{-7} Torr. This vacuum is achieved by a 6" diffusion pump coupled with a mechanical pump. The residual gas, as well as the sample purity, are controlled by the use of a commercial mass spectrometer. All metal surfaces inside the vacuum chamber are coated with colloidal graphite in order to reduce the background due to secondary electrons. The energy loss scale is calibrated by introducing helium which has a well known transition at 21.22 eV. The procedure for obtaining the electron energy loss spectra using the Möllenstedt analyzer is as follows: first the energy of the incident electrons is fixed to some value E_0 (≅ 1 keV) and then the energy loss spectrum (EELS) is recorded. This procedure is repeated many times until a good signal to noise ratio is obtained. After acquisition, the spectra are transferred to a micro-computer (IBM-PC). The correction due to electrons scattered by the background gas is made by subtracting the background spectrum from the spectrum obtained by using crossed beams collision geometry. The background spectrum is acquired by the same experimental conditions, but with the gas sample being introduced by a side flange far away from the scattering center. One more experimental correction is also introduced in data treatment and is related to the Kollath[7] correction. This corrects the transmission efficiency of the Möllenstedt analyzer.

The experimental uncertainties in the relative intensity measurements are estimated to be as follows: for our angular resolution (0.23°) the uncertainties are 20% for $\theta < 4°$

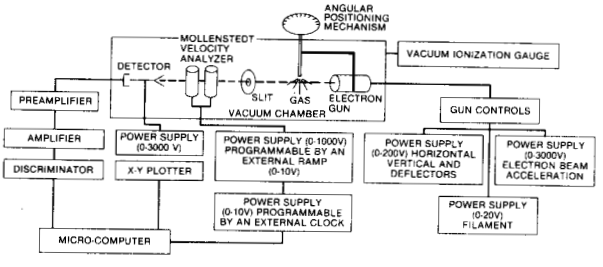

Figure 1. Schematic of the electron energy loss spectrometer.

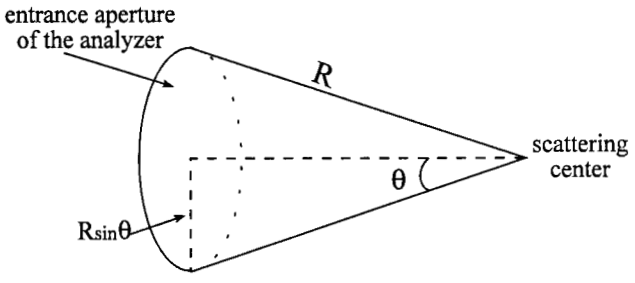

Figure 2. Solid angle subtended by the analyzer.

and 15% for $\theta > 4°$ respectively; statistical uncertainty is 3.5% (for about 2300 counts at the peak); pressure fluctuation is = 0.5% ; primary beam fluctuation is 1%. Consequently, the estimated overall uncertainty is $\delta = \sum_i \sqrt{\delta^2} \cong$ 15% for $\theta < 4°$ and 5% for $\theta > 4°$.

The method for generating photoabsorption cross sections, derived from EELS, is described in the following section.

Method of data reduction

The electron energy loss spectrum provides intensities $I(E)$ of electrons at very small scattering angles (obtained by the present experimental set-up close to 0 degree scattering angle) relative to the direction of incident electrons. Since $I(E)$ is the continuum part of the spectrum, one can define:

$$\frac{dI(E)}{d(E)} = C_1 \frac{d}{dE}\left(\frac{d\sigma(E)}{d\Omega}\right) \quad (1)$$

where $d\sigma(E)/dE$ can be defined as the density of cross section[8], E the energy lost by the incident electron, C_1 a constant which depends on several factors[9], and $d\Omega$ the solid angle subtended by the detector.

The generalized oscillator strength, f_g ,is related to the density of cross sections by the following relation[10]:

$$\frac{df_g}{dE} = \frac{1}{2a_0^2}\left(\frac{E}{E_{at}}\right)\left(\frac{P_1}{P_2}\right)\Delta P^2 \frac{d}{dE} d\sigma \left(\frac{(E)}{d\Omega}\right) \quad (2)$$

where, $a_0 = 5{,}292 \times 10^{-2}$ nm (Bohr's radius), E is the energy loss in eV, $E_{at} = 27{,}21$ eV, P_1 and P_2 are the initial and final momenta of the scattered electrons and ΔP the vector change in the momentum of the colliding electron.

It was shown by Lassettre *et al.*[1] that as $\Delta P \rightarrow$ O the GOS approaches the optical oscillator strength even if the Born approximation does not hold. It means that our electron energy loss spectrum (EELS) can be converted into a photoabsorption spectrum. Therefore, at sufficiently small values of ΔP, one can write:

$$\frac{df_g}{dE} \equiv \frac{df_{opt}}{dE} \quad (3)$$

and

$$\frac{df_{opt}}{dE} = \frac{1}{\beta}\sigma_p(E) \quad (4)$$

where $\beta = 1.098 \times 10^{-16}$ cm^2 eV and $\sigma_p(E)$ is the photoabsorption cross section.

In practice one measures the intensity $dI(E)/d\Omega$ of scattered electrons over a finite angular region $\Delta\Omega$ and, therefore, the density of a cross section can be defined by the following relation:

$$\frac{\Delta\sigma}{\Delta\Omega} = \frac{\int_{\Delta\Omega} d\Omega \left|\frac{d\sigma}{d\Omega}\right|}{\int_{\Delta\Omega} d\Omega} \quad (5)$$

The integral in equation 5 depends on the apertures used in the detector optics, and $d\sigma/d\Omega$ varies within the angular range represented by $\Delta\Omega$.

It was shown by Huebner[11] that equation 2, for a narrow circular aperture (presently used $\Delta\Omega = 3.11 \times 10^{-4}$ sr) and at high energies E_0 ($E/E_0 \cong 0.2$) f_{opt} , can be written as:

$$\frac{df_{opt}}{dE} \alpha \int (E/R).\hat{\theta}.[\ln(1+(\hat{\theta}/\gamma)^2]^{-1} \frac{d}{d(E)} \frac{\Delta\sigma(E)}{\Delta\Omega} \quad (6)$$

$$\gamma^2 = (E/2E_0)^2(1-E/R)^{-1} \text{ for constant } E_0$$

where $\hat{\theta}$ is the acceptance angle of the detector in radians, E is the energy loss in eV, E_0 the energy of the incident electron in eV, and R a factor which converts energy units to Rydbergs (13.6 eV).

Combining equations 1, 4, and 6, one can write the following equation:

$$\sigma_p(E) \alpha \left(\frac{E}{R}\right).\hat{\theta}\,[\ln(1+(\frac{\hat{\theta}}{\gamma})^2)]^{-1} \frac{\Delta I(E)}{\Delta\Omega} \quad (7)$$

The results presented in this paper were obtained by using eq. 7. A computer program was written which converted the measured scattered intensity of electrons into $\sigma_p(E)$ as a function of energy loss. However, the constant of proportionality needed in eq. 7 is not always easy to evaluate. Therefore, the values of $\sigma_p(E)$ are relative and have to be normalized to some previously known value of $\sigma_p(E)$ at at least one photon energy E.

Results and Discussion

A typical electron energy loss spectrum for argon is shown in Fig. 3. Similar spectra were obtained for N_2 and

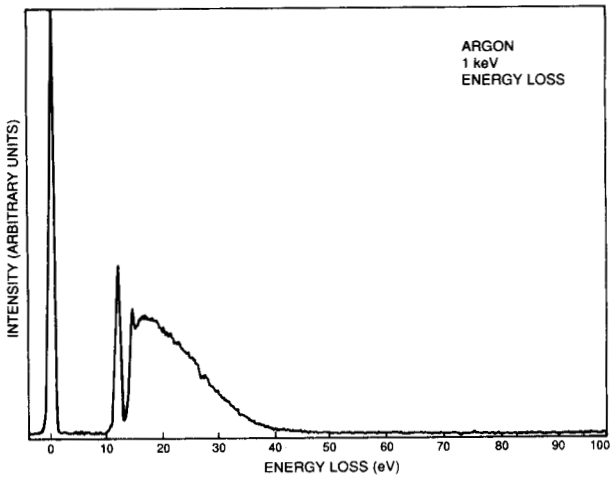

Figure 3. Electron energy loss spectrum of argon, at 1 keV.

$Si(CH_3)_4$. They were then converted to photoabsorption spectra by the method described in the previous section. They are shown in Figs. 4, 5 and 6. In the following, we present discussions on each species.

Argon

Utilizing different techniques, argon has been studied by several researchers in the past. Among them are Rustgi[12] (1963) in the wavelength region of 240 to 780 Å, Samson[13] and Cairns[14] (1964) in the wavelength region of 250 to 799 Å, Cairns and Samson[14] (1965) in the wavelength region of 303 to 799 Å, Starr and Leowenstein[15] (1972) at 584 Å, and Brolley *et al.*[16] (1973) at 584 Å. A high resolution study ($\Delta\lambda \cong 0.5$ Å) was performed by Carlson *et al.*[17] (which showed structure in the cross section data between 400 Å and 500 Å). Due to poor resolution of the present technique this structure is not seen in our data. Their results are not presented here, but are in excellent agreement with the values of Samson. It is clear from Fig. 4, that the various results agree very well with each other. Therefore, we chose ionization cross section of Ar at 21.22 eV (584 Å) measured by Samson to normalize the present relative values of cross sections. Our results, although normalized at one wavelength, are in excellent agreement with Samson's values over the entire wavelength range covered by the present experiment. This shows that the present technique and method is capable of providing reliable cross section values.

Table 1 presents the numerical values of cross sections as a function of photon energy in the photon energy range from 10 to 50 eV.

Nitrogen

Although several investigators have measured N_2 since the very first work by Hopfield[18] (1930), there are large discrepancies in published values. Just to cite a few, the photoabsorption cross section for this molecule has been measured by Weissler *et al.*[19] (1952) in the wavelength region between 300 and 1300 Å, Curtis[20] (1954) measured in the wavelength region between 150 and 1000 Å, Watanabe and Marmo[21] (1956) from 850 to 1500 Å, Huffman *et al.*[22] (1963) from 580 to 1000 Å, Cook and Metzger[23] (1964) measured from 600 to 1000 Å, Samson and Cairns[24] (1964) from 303 to 1037 Å, and again[25] in 1965 from 200 to 550 Å, Starr and Leowenstein[15] (1972) and Brolley *et al.*[16] (1973) measured them at the wavelength of 584 Å. In 1976, Starr[26] performed a series of measurements for different gases, including N_2 at wavelengths of 1302, 1304, 1306 Å. In a recent paper, Samson *et al.*[27] (1987) extended their measurements over the wavelength region from 660 to 796 Å. For the sake of comparison we have chosen a few of them and present them in Fig. 5 along with our results. The present values of relative cross sections were normalized to the results of Samson and Cairns[25] at a photon energy of 21.22 eV (586 Å). Within the error limits of the

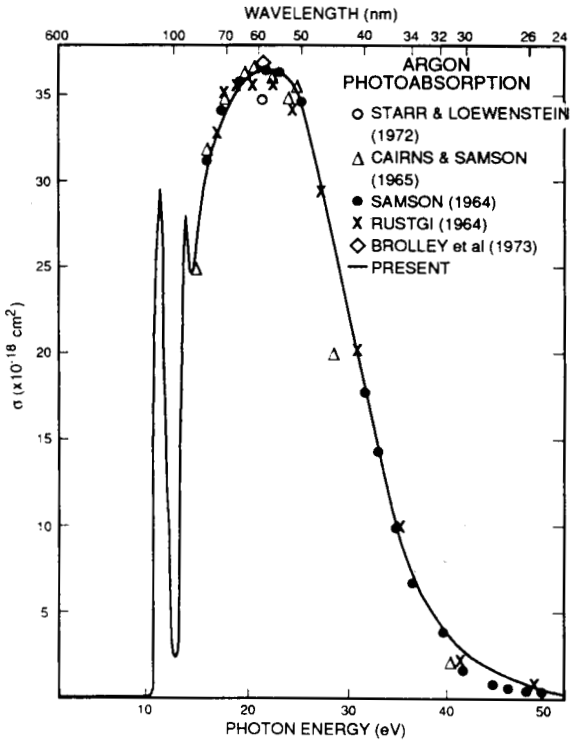

Figure 4. Photoabsorption cross sections of argon in the energy range of 10 to 50 eV.

Table 1. Normalized values of photoabsorption cross sections for argon as a function of photon energy in the energy range of 10 to 50 eV.

Photon Energy, eV	σ(x 10^{-18} cm^2)
10	0
12	29.56
14	18.08
16	29.56
18	34.08
20	35.82
22	36.52
24	35.99
26	32.86
28	28.17
30	22.78
32	17.21
34	12.52
36	8.17
38	5.56
40	3.99
45	1.56
50	0.69

Table 2. Normalized values of photoabsorption cross sections for nitrogen as a function of photon energy in the energy range of 10 to 50 eV.

Photon Energy, eV	σ(x 10^{-18} cm^2)
10	0.34
12	0.29
14	16.80
16	3.86
18	4.33
20	4.12
22	3.91
24	4.03
26	4.28
28	4.07
30	4.12
32	4.03
34	3.82
36	3.40
38	3.02
40	2.77
45	2.39
50	1.85

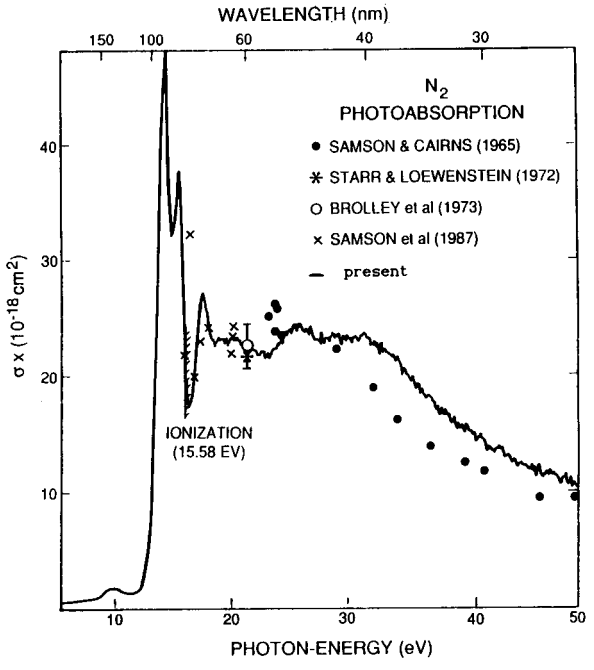

Figure 5. Photoabsorption cross sections of nitrogen in the energy range of 10 to 100 eV.

present experiment the agreement is satisfactory. Table 2 presents our normalized cross sections.

Examination of published values of photoabsorption cross section data reveals large disagreements, and the catalogued values differ by orders of magnitude. This lack of agreement can be mainly attributed to insufficient wavelength resolution in many experimental techniques, especially in the region exhibiting structure. In the continuum region, after the first ionization potential (15.58 eV), the photoabsorption cross section varies slowly with the wavelength in such a way that the measurements will not differ very much if they are made by the use of a continuum source. Measurements of cross sections should be nearly independent of bandwidth and would be expected to show good agreement. On the other hand, if absorption is in a region in which the cross section varies rapidly with the wavelength, large discrepancies are to be expected whether a continuum or a line source is used. This effect is due to the fact that the radiation absorption is likely to be dependent on the distribution of radiation within the line source or the bandwidth of the monochromator, if a continuum source is used. Studies were made[28] of the effect of the instrumental bandwidth on the measured absorption cross section and line shapes in the ultraviolet. In the case of N_2, the above factors should be taken into account when comparing data obtained by different methods.

Tetramethylsilane

This molecule has been previously studied by Sodhi *et al.*[29] who also employed the same EELS technique as the present one. However, their resolution was better than ours. Therefore, they observed structure in their spectrum obtained at 3 keV incident electron energy and a zero degree scattering angle. However, recent photoabsorption cross section[30] measurements in the wavelength region between 55 nm and 95 nm with the same wavelength resolution as that of Sodhi *et al.* did not show any such structure.

We normalized our relative values of cross sections with the cross section value of reference 30 at 65 nm. The resulting cross sections for wavelengths between about 12 nm and 206 nm are shown in Fig. 6. As it is clear from this figure, between 55 Å and 75 Å the agreement in the shapes of the two curves is excellent. However, at longer wavelengths the two results differ considerably from each other. We suspect that at longer wavelengths the conversion of photon energy into wavelength is quite sensitive to small errors in the measurement of energy loss which is equal to the photon energy. In addition, at longer wavelengths the intensity varies very rapidly. Therefore, small errors in the energy loss can result in large errors in the intensity of scattered electrons. We are confident that the results presented are accurate at shorter wavelength to within 20%. They are tabulated in Table 3. In this table we have expressed cross section values to the second decimal

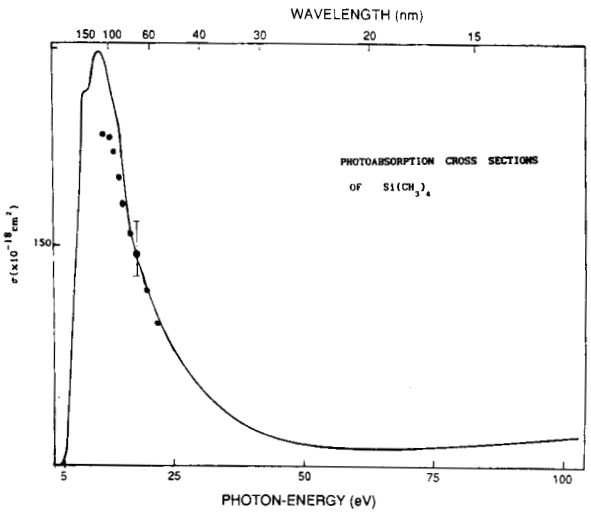

Figure 6. Photoabsorption cross sections of tetramethylsilane in the energy range of 20 to 50 eV.

Table 3. Normalized values of photoabsorption cross sections for tetramethylsilane as a function of photon energy in the energy range of 5 to 100 eV.

Photon Energy, eV	σ (x10 $^{-18}$ cm^2)
6	0.43
7	8.67
8	43.57
9	81.75
10	116.42
12	157.78
14	226.73
16	201.86
18	156.64
20	125.40
22	102.00
24	80.30
26	64.40
28	50.10
30	40.90
35	21.70
40	12.90
45	8.10
50	5.10
55	3.40
60	2.50
65	1.50
70	1.10
75	0.47
80	0.35
85	0.21
90	0.087
95	0.087
100	0.043

place, which appears to be unreasonable since our quoted accuracy is only 20%. The presented values are obtained by digitizing the smooth curve of Fig. 6. Our previous experience with modellers has been that they prefer the tabulated data in the present form in order to incorporate it into their computer codes.

Conclusions

We conclude that the technique of EELS can generate photoabsorption data in a large wavelength range without the need of expensive photoabsorption data. However, the resolution is poor and at longer wavelengths many details can be missed. For the first time we have generated photoabsorption cross sections for TMS for an extended range of wavelengths.

Acknowledgments

This work was performed under the auspices of international bilateral cooperation between the CNPq (Brazil) and the NSF (USA). The authors would like to thank their sponsors for funding this work and for providing travel grants for both.

References

1. E.N. Lassettre, A. Skeberle and M.A. Dillon, *J. Chem. Phys.* **50**, 1829 (1969).
2. G.G.B. de Souza and A.C.A. Souza, *J. Phys.* **E**: *Scient. Instrum.* **18**, 1037 (1985).
3. A.C.A. Souza, S.K. Srivastava and G.G.B. de Souza, "Photoabsorption Cross Sections for Ammonia, Acetylene and Methane in the Photon Energy Range of 5 to 100 eV", to be published.
4. G.G.B. de Souza, M.C.A. Santos and E.M.A. Peixoto, *Optik* **53**, 405 (1979).
5. H.M. Boechat Roberty, PhD. Thesis, Brazilian Center of Physics Research (CBPF), Rio de Janeiro, Brazil, 1990.
6. H. Semat and J.R. Albright, *Introduction to Atomic and Molecular Physics* (Holt Rinehart Winston, 1972).
7. R. Kollath, *Ann. Phys.* **27**, 121 (1937).
8. M. Inokuti, *Rev. Mod. Phys.* **43**, 297 (1971).
9. S.K. Srivastava, A. Chutjian and S. Trajmar, *J. Chem. Phys.* **63**, 2659 (1975).
10. C.E. Kuyatt, *Methods of Experimental Physics* (B. Bederson and W.L. Fite, Academic Press, NY, 1968) **47**, 1.
11. R.H. Huebner, R.J. Celotta, S.K. Mielckzarek and C.E. Kuyatt, *J. Chem. Phys.* **59**, 5434 (1973).
12. O.P. Rustgi, *J. Opt. Soc. Am.* **54**, 464 (1964).
13. J.A.R. Samson, *J. Opt. Soc. Am.* **54**, 420 (1964).
14. R.B. Cairns and J.A.R. Samson, *J. Geophys. Res.* **70**, 99 (1965).
15. W.L. Starr and M. Leowenstein, *J. Geophys. Res.* **77**, 4790 (1972).

16. J.E. Brolley, L.E. Porter, R.H. Sherman, J.K. Theobald and J.C. Fong, *J. Geophys. Res.* **78**, 1627 (1973).
17. R.W. Carlson, D.L. Judge, M. Ogawa and L.C. Lee, *Appl. Phys.* **12**, 409 (1973).
18. J.J. Hopfield, *Phys. Rev.* **36**, 789 (1930) and *Astrophys. J.* **72**, 133 (1930).
19. G.L. Weissler, P. Lee and E.I. Mohr, *J. Opt. Soc. Am.* **42**, 84 (1952).
20. J.P. Curtis, *Phys. Rev.* **94**, 908 (1954).
21. K. Watanabe and F.F. Marmo, *J. Chem. Phys.* **25**, 965 (1956).
22. R.E. Huffman, Y. Tanaka and J.C. Larrabee, *J. Chem. Phys.* **39**, 910 (1963).
23. G.R. Cook and P.H. Metzger, *J. Chem. Phys.* **41**, 321 (1964).
24. J.A.R. Samson and R.B. Cairns, *J. Geophys. Res.* **69**, 4583 (1964).
25. J.A.R. Samson and R.B. Cairns, *J. Opt. Soc. Am.* **55**, 1035 (1965).
26. W.L. Starr, *J. Geophys. Res.* **81**, 3363 (1976).
27. J.A.R. Samson, T. Masuoka, P.N. Pareek and G.C. Angel, *J. Chem. Phys.* **86**, 6128 (1987).
28. R.D. Hudson and V.L. Carter, *J. Opt. Soc. Am.* **58**, 227 (1968).
29. R.N.S. Sodhi, S. Daviel, C.E. Brion and G.G.B. de Souza, *J. Electron Spectrosc. Rel. Phen.* **35**, 45 (1985).
30. K. Kameta, M. Ukai, T. Numazawa, N. Terazawa, I. Chikahiro, N. Kouchi and Y. Hatano, *J.C.P.* **99**, 2487 (1993).